Desalination and Water Treatment
www.deswater.com
doi: 10.1080/19443994.2014.923213

54 (2015) 3566–3574
June

Taylor & Francis
Taylor & Francis Group

Filtration performance comparison of a metal membrane and an organic membrane in bioreactor

Yuanhua Xie[a,*], Xianjin Li[a], Tianyu Chai[a], Jungang Ren[a], Lan Ding[b], Yaonan Zhu[c], Jin Han[a], Tong Zhu[a]

[a]*School of Mechanical Engineering and Automation, Northeastern University, 3-11, Wenhua Road, Heping District, Shenyang 110004, China, Tel./Fax: +86 24 83679926; email: yhxie@mail.neu.edu.cn (Y. Xie)*
[b]*Anshan Environmental Monitoring Center, 3-1, Changqing Road, Tiedong District, Anshan 114004, China*
[c]*College of Information Science and Engineering, Northeastern University, 3-11, Wenhua Road, Heping District, Shenyang 110004, China*

Received 15 January 2014; Accepted 14 March 2014

ABSTRACT

A metal membrane and a polyethersulfone (PES) membrane were compared in this study. The surface morphology, inherent resistance, and critical flux of the membranes were first investigated. The two membranes were then placed in an activated sludge reactor to treat municipal sewage. The two membranes showed similar removal efficiencies of chemical oxygen demand (COD), ammonia, and total nitrogen (TN). The average effluent COD removal efficiencies, effluent ammonia, and effluent TN removal efficiencies were approximately 94.00%, 0.19 mg/L, and 28.22%, respectively. The metal membrane showed lower inherent membrane resistance of $0.27 \times 10^{11}\ m^{-1}$, higher critical flux of $0.7\ m^3/(m^2\ d)$, higher anti-fouling ability, and slower transmembrane pressure increasing rate compared with the PES membrane. The main fouling mechanism of the metal membrane was cake formation, whereas that of the PES membrane was pore blocking. The metal membrane was easy to recover after fouling. The results of the study suggest that the metal membrane can be potentially applied in a membrane bioreactor.

Keywords: Filtration performance; Membrane bioreactor; Membrane fouling; Metal membrane; Organic membrane

1. Introduction

The widespread application of membrane bioreactors (MBRs) is restricted by its key element, membrane, due to several factors. First, the high cost of membranes result in an increase in construction investment. Second, the short lifetime of membranes entails huge operating cost. Finally, membrane fouling during operation leads to low flux, complex maintenance, and increased cost [1–3].

Membrane materials that are commonly used in MBRs can be classified into three major categories: polymeric, inorganic (ceramic), and metal [4]. Polymeric membranes, such as polyolefin, polyacrylic acid, polysulfone, polyvinyl alcohol, and polyimide [5], are easily manufactured at a relatively low cost. However,

*Corresponding author.

Presented at the 5th IWA-ASPIRE Conference, 8–12 September 2013, Daejeon, Korea

these membranes have poor adaptability to different substances, low resistance against chemical corrosion, and weak mechanical strength. These disadvantages make the recovery of decreased permeate flux after heavy fouling very difficult [6]. Zhang et al. studied the affinity between extracellular polymeric substance and three polymeric membranes, and discovered that the affinity capability came in the following order: polyacrylonitrile (PAN) < polyvinylidene fluoride (PVDF) < polyethersulfone (PES) [7]. The result suggested that the PAN membrane was the most resistant to fouling. Zhu et al. reported that the PES membrane has better capability than the PVDF membrane in the treatment of domestic wastewater [8].

Ceramic membranes have been widely used given their good chemical reliability, reasonable mechanical strength, high removal efficiency, and strong tolerance for cleaning [4,9]. However, the pore size control, membrane unit sealing, and frangibility of this membrane type need improvement. Metal membranes have also been used in MBRs given their good filtration performance, fine fouling recovery performance, high mechanical strength, and high tolerance to oxidation and high temperatures [5,10,11]. Zhang et al. compared the surface morphology of a polyethylene (PE) membrane and a stainless steel membrane and found that the stainless steel membrane was easier to recover after fouling than the PE membrane [10]. Kang et al. applied a polypropylene (PP) membrane and a zirconia skinned carbon membrane to treat alcohol distillery wastewater in an anaerobic bioreactor [12]. The major filtration resistance of the PP membrane was found to be cake resistance, whereas that of the zirconia skinned membrane was internal resistance.

The present study compared the filtration performance of a metal membrane and an organic membrane in an aerobic bioreactor that was used to treat synthetic domestic sewage under the same operating conditions. The membrane surface morphology was observed by a scanning electron microscope (SEM). The inherent resistance and critical flux of the membranes were investigated subsequently. The removal efficiencies of chemical oxygen demand (COD), ammonia, and total nitrogen (TN) as well as the transmembrane pressure (TMP), fouling mechanism, and membrane cleaning effect were compared under continuous filtration experiment.

2. Materials and methods

2.1. Membrane units

The metal membrane unit and the organic membrane unit were both flat membranes with a pore size of 0.4 μm, a filtration area of 0.12 m^2 (2 sides × 0.3 m × 0.2 m), and the same outline size. The metal membrane was made of stainless steel and was provided by Hitachi Metals Co., Japan. The organic membrane was made of PES and was purchased from Wuhan Jiecheng Co., China.

2.2. Experimental system

The effective volume of the aeration tank was 30 L under the combination control of water level sensor and influent pump (Fig. 1). The sandwich membrane module, in which three polymethyl methacrylate plates were used to hold one stainless steel membrane sheet and one PES membrane sheet (only two polymethyl methacrylate plates and one membrane are shown in Fig. 1), was set vertically in the aeration tank. The ports of the two membrane sheets were connected to two constant flow suction pumps. Pressure meters were set to monitor the TMPs. A diffuser was installed below the membrane module to blow out the biofilm cake that would form on the membrane surface and to supply oxygen to the activated sludge bacteria. The aeration flow could be adjusted by the air flow meter.

2.3. Operation methods

A synthetic domestic sewage with a BOD_5/COD (biochemical oxygen demand in 5 d [BOD_5]) ratio of about 0.74, COD:N:P = 100:10:1, and a nearly neutral pH was used as influent [5]. The seed sludge was taken from a lab-scale fill-and-draw batch reactor

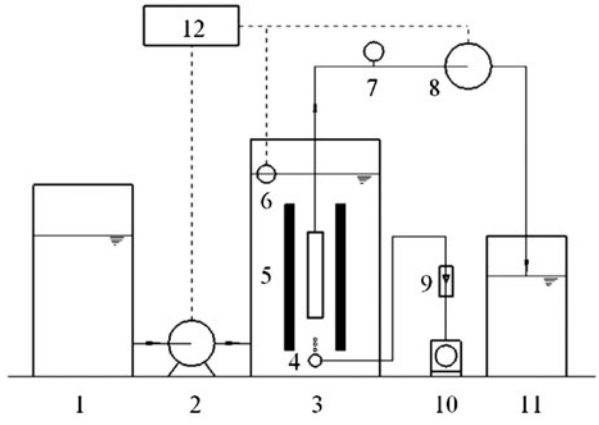

Fig. 1. Schematic diagram of the MBR system. 1—Influent tank, 2—influent pump, 3—aeration tank, 4—diffuser, 5—membrane module, 6—water lever sensor, 7—pressure meter, 8—suction pump, 9—air flow meter, 10—air pump, 11—effluent tank, and 12—control panel.

(Northeastern University, China), and the initial mixed liquor suspended solids (MLSS) concentration was set at about 12,000 mg/L. The temperature was maintained at about 20 °C, and the aeration flow rate was kept at 20 L/min by the air flow meter. These parameters were used for both the membrane critical flux test and the continuous filtration experiment.

The continuous filtration experiment lasted 45 d. Intermittent suction was applied to release the membrane fouling. The working cycle was 6 min suction plus 1 min pause. The membrane permeate flux was set at 0.4 $m^3/(m^2\,d)$. Offline cleaning with 0.1% NaClO solution, whose pH was adjusted to about 12 using NaOH, was carried out when the TMP exceeded 20 kPa.

2.4. Analytical and calculation methods

BOD_5, COD, TN, total phosphorus, and MLSS were measured by the standard methods [13]. Ammonia was measured by the OPP method [14]. pH was measured by a sensION378 meter (Hach, USA). The membrane surface morphology was observed by SSX-550 SEM (Shimadzu, Japan).

The TMP was continuously measured by a pressure meter, and filtration resistance R was calculated by the following equation:

$$R = \mathrm{TMP}/(\mu J) \tag{1}$$

where TMP (Pa) is the transmembrane pressure, μ (Pa s) is the viscosity of the permeated liquor, J ($m^3/(m^2\,d)$) is the permeate flux, and R ($1/m$) is the filtration resistance.

The step flux method [15] was used to determine the membrane critical flux. The tested flux range was 0.3–1.1 $m^3/(m^2\,d)$, the flux step was 0.1 $m^3/(m^2\,d)$, and the running time of each step was 30 min. Mechanical cleaning was performed after each test step to ensure the same initial membrane condition.

The total filtration resistance R_t consisted of four parts:

$$R_t = R_m + R_p + R_c + R_i \tag{2}$$

where R_m ($1/m$) is the inherent membrane resistance, R_p ($1/m$) is the polarization layer resistance, R_c ($1/m$) is the cake resistance, and R_i ($1/m$) is the internal resistance. R_t is calculated by the final permeate flux and the TMP at the end of the operation in MBR by Eq. (1). R_m is obtained by the filtration of the new membrane with pure water before operation. Filtration of the operated membrane with tap water yields R_0; $R_t - R_0 = R_p$. Filtration of the operated membrane with pure water after removing the cake layer by sponge scrubbing yields R_1; $R_0 - R_1 = R_c$. R_i can be obtained using Eq. (2).

3. Results and discussion

3.1. Comparison of membrane inherent performance

3.1.1. Membrane surface morphology

Membrane fouling was affected by membrane surface morphology, including pore size, pore size distribution, surface roughness, and porosity. When membrane pore size was close to the microparticle size in mixed liquor, the microparticle blocked or was adsorbed by membrane pores easily, thereby causing severe fouling [16]. With the increase in membrane surface roughness, the contaminants in mixed liquor were easily adsorbed or deposited on the membrane surface and were thus difficult to be removed by cross-flow [17].

Figs. 2 and 3 show the SEM images of the stainless steel membrane and the PES membrane, respectively. The stainless steel membrane comprised a mesh support layer, a powder support layer, and a powder filtration layer. The filtration performance was mainly determined by the pore size of the powder filtration layer. The powder filtration layer had a maximum pore size of 2.28 μm, a minimum pore size of 1.19 μm, a 50% median diameter of 1.35 μm, and a porosity of 19.8%. The PES membrane comprised a series of interwoven fibers that formed a complex spatial network structure. Its surface pore size could not be measured accurately, but its pore size magnitude was determined to be 10 μm via qualitative analysis.

The pore sizes of the stainless steel membrane and the PES membrane differed by one order of magnitude, but the nominal pore size of both membranes was 0.4 μm. These characteristics are explained as follows. The filtration of the stainless steel membrane occurred on its surface layer, and the contaminants were mainly trapped on the membrane surface. The removal of contaminants in the PES membrane was the effect of multiple trapping resulting from the special spatial network structure of this membrane. Contaminants easily penetrated the membrane and were easily captured, thus causing irreversible pollution and the formation of an auxiliary filtration layer. Finally, the nominal pore sizes of both membranes were assumed to be the same.

The large pore size of the PES membrane also increased its surface roughness. As shown in Figs. 2

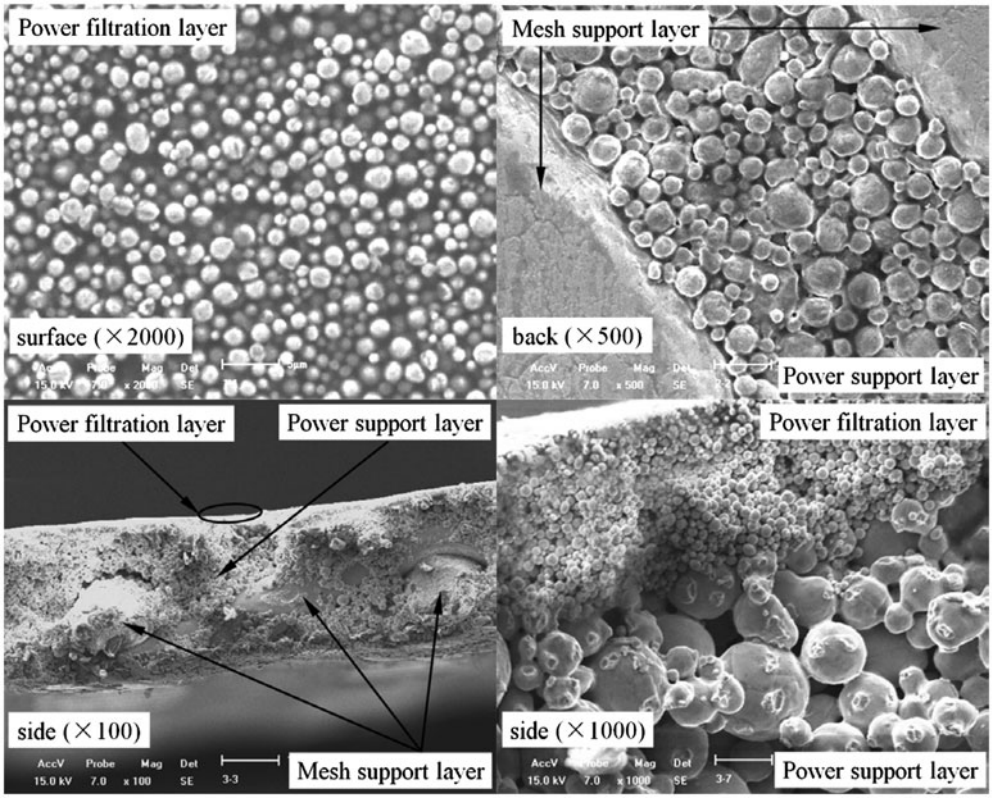

Fig. 2. SEM images of stainless steel membrane.

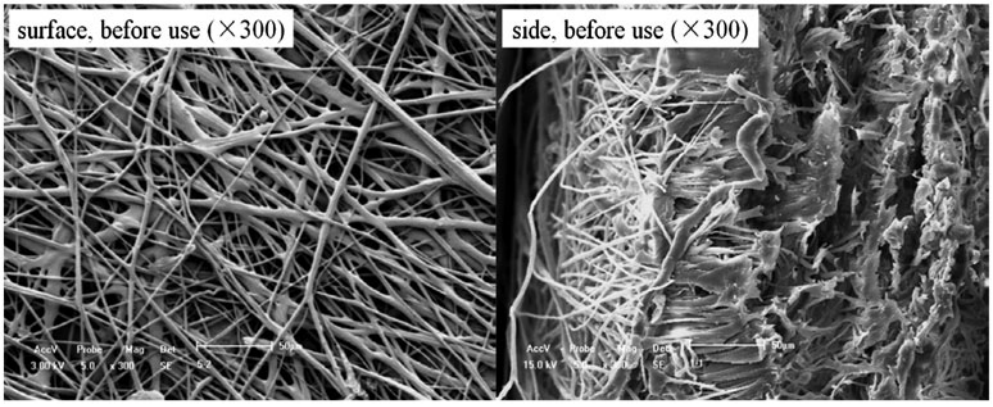

Fig. 3. SEM images of PES membrane.

(side) and 3 (side), the surface of the stainless steel membrane was significantly smoother than that of the PES membrane. As a result, contaminants were adsorbed by or deposited on the surface of the PES membrane easily, thereby forming a filtration cake layer and increasing membrane fouling and filtration resistance. Zhang et al. proved that a much heavier fouling of PES membranes had taken place due to its relatively high roughness [7].

3.1.2. Inherent membrane resistance

Inherent membrane resistance was measured by filtration with tap water at 20°C and then calculated using Eq. (1). Fig. 4 shows the relationship between the TMP and the membrane permeate flux. The inherent resistance of the stainless steel membrane was $0.27 \times 10^{11}\ m^{-1}$, whereas that of the PES membrane was $1.06 \times 10^{11}\ m^{-1}$. Despite its smaller pore size, the

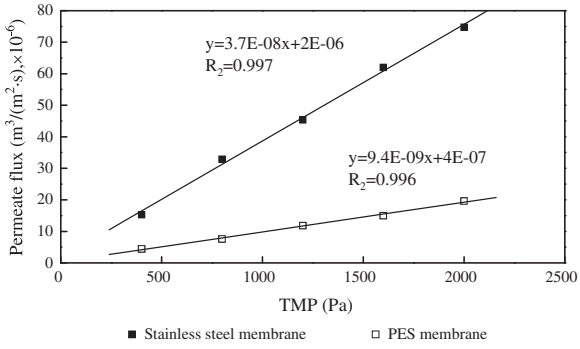

Fig. 4. Permeability performances of stainless steel membrane and PES membrane.

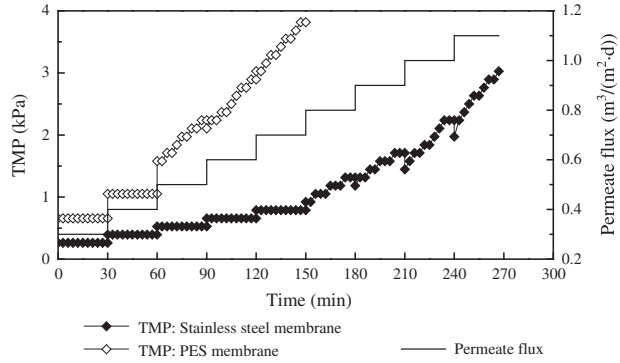

Fig. 5. TMP and permeate flux vs. time.

stainless steel membrane showed smaller inherent resistance compared with the PES membrane. The reasons could be the following: the main filtration layer of the stainless steel membrane was extremely thin, and most of the membrane thickness comprised a support layer with large pore size and porosity. This characteristic reduced the total filtration resistance. The special spatial network structure of the PES membrane increased the filtration channel length, thus resulting in high filtration resistance. In addition, the high hydrophilia of the stainless steel membrane might have also contributed to its low inherent resistance [18].

3.1.3. Membrane critical flux

A high operating flux corresponds to high water productivity per unit area of a membrane and to a small membrane investment. However, a high operating flux will cause serious membrane fouling, thus increasing the frequency of membrane cleaning and running costs. Therefore, an appropriate operating flux must be established to balance the membrane investment cost with the membrane service life and system running cost. Critical flux was first presented by Field et al. [19] and has been widely applied in the development of slow membrane fouling and in the balance among membrane investment, membrane life, and running cost.

Fig. 5 shows the changes in the TMP and membrane permeate flux with time in the measurement of critical flux. The critical flux of the stainless steel membrane was 0.7 $m^3/(m^2 d)$, whereas that of the PES membrane was only 0.4 $m^3/(m^2 d)$. This difference could be attributed to the large pore size and weak hydrophilia of the PES membrane. These characteristics enabled the microparticles to be adsorbed easily into the membrane pores, thus reducing the filtration channel. The high surface roughness of the PES membrane that resulted in the relatively strong adsorption of contaminants and poor cleaning effect by cross-flux might be another reason.

3.2. Removal efficiencies

Figs. 6 and 7 show the changes in the COD and nitrogen removal efficiencies of the two membranes with time. During the whole operation process, both membrane effluents showed good COD removal efficiencies. The average COD removal efficiencies were 94.86% for the stainless steel membrane and 93.86% for the PES membrane. The removal efficiencies of the two membranes were approximately equal because they shared the same activated sludge reactor and the same nominal pore size. The NH^{4+}–N and TN removal efficiencies of the two membranes were also approximately the same. The average NH^{4+}–N concentration in effluent was very low (0.19 mg/L), and the average TN removal efficiency was 28.22%. The low NH^{4+}–N concentration in effluent resulted from

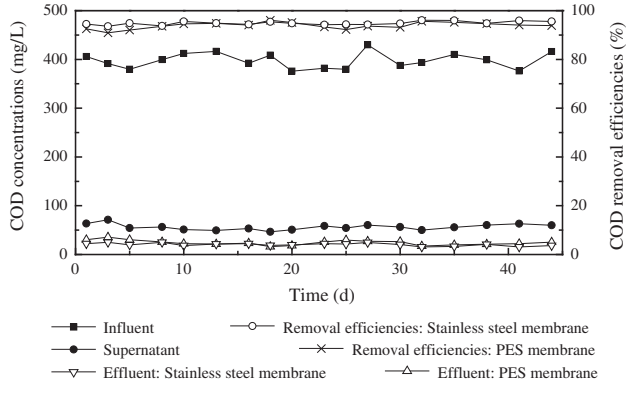

Fig. 6. Daily changes in COD removal efficiencies.

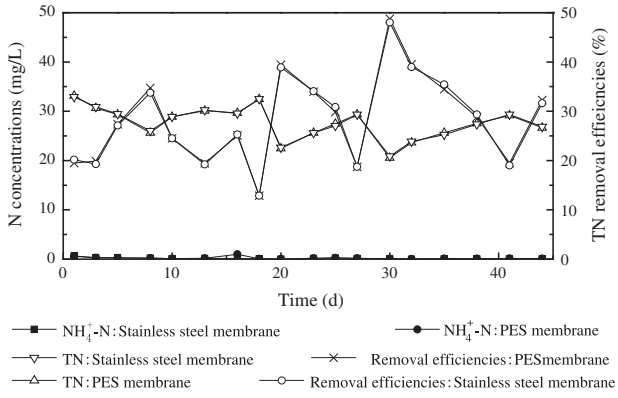

Fig. 7. Daily changes in N and TN removal efficiencies.

the interception effect of the membrane on the nitrifier and nitrosobacteria [5,10]. The removal of TN was mainly the result of sludge breeding and sludge drawing of the bioreactor.

3.3. Membrane fouling mechanism

Fig. 8 shows the daily changes in the TMP of the stainless steel membrane and the PES membrane. During the 45 d operation period, the TMP of the PES membrane increased significantly faster than that of the stainless steel membrane. The TMP of the PES membrane reached 21.05 and 24.47 kPa within 21 and 24 d, respectively. By contrast, the TMP of the stainless steel membrane only reached 20.92 kPa after 45 d of continuous operation. Hence, the stainless steel membrane had higher anti-fouling ability than the PES membrane because of its inherent performance. The operation flux of the two membranes was less than their critical flux. However, membrane fouling occurred continually, and the filtration channels were blocked gradually in actual operation, thus causing the continuous reduction of

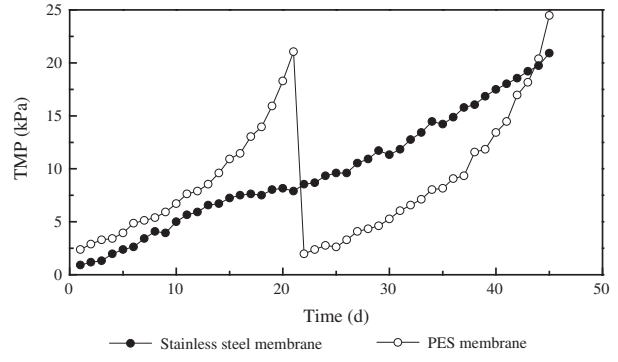

Fig. 8. Daily changes in TMP.

real critical flux. Once the operational flux exceeded the real critical flux, membrane fouling developed quickly, and the TMP increased rapidly [20].

Table 1 shows the filtration resistance composition of the two membranes measured in the offline cleaning process. The values of the total filtration resistance R_t were almost the same under different offline cleaning processes. Thus, the proportion changing trends under each resistance section in Table 1 could also represent real trends. Within four sections of the membrane filtration resistance, the inherent membrane resistance R_m accounted for the smallest proportion, that is, 0.6% for the stainless steel membrane and 2.0–2.3% for the PES membrane. The proportion of the polarization layer resistance R_p was slightly higher than the inherent membrane resistance at a range of 4.5–8.3%. The polarization layer resistance of the PES membrane was higher than that of the stainless steel membrane because the surface roughness of the former is higher, thus resulting in a relatively thick and stable concentration polarization layer. As for the stainless steel membrane, the cake resistance R_c and the internal resistance R_i accounted for 63.8 and 31.0%, respectively. The cake resistance was obviously the major resistance of the stainless steel membrane. By contrast, the cake resistance R_c and the internal resistance R_i of the PES membrane accounted for 35.6–42.7% and 49.3–53.8%, respectively; internal resistance was the major resistance of this membrane.

Aryal et al. used a tubular stainless steel membrane with an average pore size of 0.3 μm to continuously filtrate a synthetic substrate for 2 d [11]. The results also showed that the cake resistance ($4.4 \times 10^{19}\ m^{-1}$) was the major resistance, followed by the internal resistance ($2.8 \times 10^{16}\ m^{-1}$) and the inherent membrane resistance ($5.4 \times 10^{12}\ m^{-1}$). Compared with my study, the cake resistance and the internal resistance were much higher than the inherent membrane resistance. It might result from the continuous filtration without pause and the short operation period of 2 d. An opposite conclusion was drawn when applying a PP membrane and a zirconia skinned carbon membrane to treat alcohol distillery wastewater in an anaerobic bioreactor [12]. The major resistance of the PP membrane and the inorganic membrane were found to be the cake resistance and the internal resistance, respectively. The composition of the feed wastewater (be rich of Mg^+, NH_4^+, PO_4^{3-}, and easy to generate $MgNH_4PO_4{\cdot}6H_2O$) and the anaerobic condition were considered as the main reasons.

As mentioned previously, the filtration of the stainless steel membrane mainly relied on surface screening. That is, the particles larger than the membrane pore size were intercepted, the smaller particles went

Table 1
Composition of filtration resistance

Membrane type	Day	R_m		R_p		R_c		R_i		R_t	
		$m^{-1}, \times 10^{11}$	%	$m^{-1}, \times 10^{11}$	%	$m^{-1}, \times 10^{11}$	%	$m^{-1}, \times 10^{11}$	%	$m^{-1}, \times 10^{11}$	%
PES	21	1.06	2.3	3.82	8.3	16.39	35.6	24.81	53.8	46.08	100
PES	45	1.06	2.0	3.18	5.9	22.89	42.7	26.43	49.3	53.56	100
Stainless steel	45	0.27	0.6	2.08	4.5	29.23	63.8	14.21	31.0	45.79	100

Note: R_m: the inherent membrane resistance, R_p: the polarization layer resistance, R_c: the cake resistance, R_i: the internal resistance, and R_t: the total filtration resistance.

through, and only few particles whose sizes were close to the membrane pore size were adsorbed by or trapped inside the membrane. On the contrary, the PES membrane could capture a wide range of particles with a variety of filtration mechanisms because of its complex spatial network structure. For example, the PES membrane captured particles larger than the membrane pore size through multiple screening, caught large particles in inertial movement through collision, and captured small particles in random movement through Brown diffusion interception. Consequently, a large amount of particles remained in the interior of the PES membrane, quickly leading to the development of membrane fouling. These conditions resulted in the cake resistance and internal resistance being the dominant resistances of the stainless steel membrane and the PES membrane, respectively. The same conditions also led to the TMP of the PES membrane increasing faster than that of the steel membrane.

3.4. Membrane cleaning

Many cleaning methods are currently available; examples include physical methods of backwashing, ultrasonic, mechanical sponge scrubbing, high-pressure steam, and high pressure water; and chemical methods using strong acid, strong alkali, oxidant, and surfactant [4–6,10,12,16,21]. According to the nature of membrane material, strong cleaning methods, such as high-pressure steam, ozone, and various combination methods, were adoptable for the stainless steel membrane. Therefore, the membrane fouling of the stainless steel membrane could more easily be controlled compared with that of the PES membrane. Zhang et al. also reported that the stainless steel membrane was easier to clean than the organic one [10].

Table 2 shows the membrane filtration resistance before and after 4 h of continued aeration on the 44th day. The continued aeration had superior fouling removal effect on the stainless steel membrane because of the following reasons: the cake layer on the surface of this membrane was relatively thick, the binding force between the cake layer and the surface of the stainless steel membrane was relatively weak because of its low roughness, and the cake layer was easily removed by membrane surface cross-flow when air aerated. Table 1 shows that the cake resistance proportion of the stainless steel membrane is greater than that of the PES membrane. Therefore, the fouling removal effect on the stainless steel membrane by mechanical sponge scrubbing was also better than that on the PES membrane.

3.5. Application prospects of the stainless steel membrane

Compared with the organic membrane, the manufacturing process of the stainless steel membrane is relatively complex, leading to high price. According to the data provided by Hitachi Metals Co., Japan, the price of the stainless steel membrane sheet is about 10 times of the PES membrane sheet in this study. It will result in high initial investment for the MBR system that using the stainless steel membrane. The stainless steel membrane sheet (about 894 g) is also heavier than the PES membrane sheet (about 436 g) in

Table 2
Cleaning effect of continued aeration on membrane fouling for the two membranes

Membrane type	Stainless steel membrane	PES membrane
Filtration resistance before continued aeration ($m^{-1}, \times 10^{11}$)	43.20	44.64
Filtration resistance after continued aeration ($m^{-1}, \times 10^{11}$)	38.30	41.18
Reduction proportion of membrane filtration resistance (%)	11.33	7.75
Time for membrane resistance to increase to original level (h)	4.3	1.6

this study. It will increase the transportation cost and the operation cost to some extent.

The shortcoming of the stainless steel membrane in price and weight could be balanced by its flowing advantages. The above comparative study proved that the stainless steel membrane had low intrinsic resistance and high critical flux, and thus could be run under high permeate flux in actual operation. It indicated that the required membrane amount for the same treatment scale would decrease when using the stainless steel membrane. Accordingly, several benefits could be achieved as less initial membrane investment, smaller MBR system footprint, and less initial civil construction investment is needed. The stainless steel membrane in this study was the production of Hitachi Metals Co., Japan in bench scale. Its price will also decrease along with the increasing production scale.

The operation life of the organic membrane is about 3–5 years, whereas that of the stainless steel membrane is 10 years or more. The total membrane investment will be further reduced due to the long operation life of the stainless steel membrane, and thus, the membrane investment difference resulted from the price between the stainless steel membrane and the organic membrane will be narrowed.

The above study also proved that the stainless steel membrane had higher fouling resistance than the PES membrane. Less membrane cleaning was required in long operation process for the stainless steel membrane. The energy consumption and the operational management costs of stainless steel MBRs would be saved.

Due to the high mechanical strength, the high tolerance to oxidation and high temperatures, high resistance to corrosion, more cleaning methods, and more cleaning agents can be used against membrane fouling. The membrane flux can be recovered easily after membrane fouling.

Besides the above features, the stainless steel membrane also has the following advantages. It can be stored in a dry state, greatly reducing the maintenance and care costs. The stainless steel material can be recycled without causing environment problems. The stainless steel membrane can be used at a large temperature range (up to about 200°C) and can be used for high-temperature waste water treatment.

In brief, although the stainless steel membrane is expensive, the price shortage can be balanced by its merits in several aspects. With the further improvement of manufacturing technology, the cost of the stainless steel membrane will gradually decrease. The stainless steel membrane would be widely used in urban sewage treatment and other industrial wastewater treatment.

4. Conclusion

The inherent properties, contamination removal efficiencies, and fouling characteristics of the stainless steel membrane and the PES membrane were compared in this work. The following conclusions could be drawn:

(1) The inherent performance of the stainless steel membrane was considerably better than that of the PES membrane. The values of the inherent resistance of the stainless steel membrane and the PES membrane were $0.27 \times 10^{11}\,m^{-1}$ and $1.06 \times 10^{11}\,m^{-1}$, respectively. The values of the critical flux of the stainless steel membrane and the PES membrane under MLSS of 12 g/L were 0.7 and $0.4\,m^3/(m^2\,d)$, respectively.
(2) Given the same nominal pore size of the stainless steel membrane and the PES membrane, the COD, NH^{4+}-N, and TN removal efficiencies were similar for the two membranes.
(3) The TMP of the stainless steel membrane increased slower than that of the PES membrane under the same conditions. Furthermore, the anti-fouling ability of the stainless steel membrane was higher than that of the PES membrane. Under aerobic operation, the dominant resistance of the stainless steel membrane and the PES membrane were cake resistance and internal resistance, respectively.
(4) The membrane fouling of the stainless steel membrane could more easily be controlled compared with that of the PES membrane. The stainless steel membrane was easier to recover after fouling than the PES membrane under aerobic operation.
(5) Despite the high price, the stainless steel membrane has great advantages in permeate flux, operation life, cleaning methods, maintenance managements, and application scope. It has great potential and good prospect in urban sewage treatment and other industrial wastewater treatment.

Acknowledgment

This work was jointly supported by National Natural Science Foundation of China (No. 21107011, No. 51178098), Science and Technology Projects of Shenyang, China (No. F12-277-1-17), and the Fundamental Research Funds for the Central Universities of China (No. N100303006).

References

[1] F.G. Meng, S.-R. Chae, A. Drews, M. Kraume, H.-S. Shin, F.L. Yang, Recent advances in membrane bioreactors (MBRs): Membrane fouling and membrane material, Water Res. 43 (2009) 1489–1512.

[2] P. Le-Clech, Membrane bioreactors and their uses in wastewater treatments, Appl. Microbiol. Biotechnol. 88 (2010) 1253–1260.

[3] A.H. Birima, T.A. Mohammed, M.J.M.M. Noor, S.A. Muyibi, A. Idris, H. Nagaoka, J. Ahmed, L.A.A. Ghani, Membrane fouling in a submerged membrane bioreactor treating high strength municipal wastewater, Desalin. Water Treat. 7 (2009) 267–274.

[4] H.J. Lin, W. Peng, M.J. Zhang, J.R. Chen, H.C. Hong, Y. Zhang, A review on anaerobic membrane bioreactors: Applications, membrane fouling and future perspectives, Desalination 314 (2013) 169–188.

[5] Y.H. Xie, T. Zhu, C.H. Xu, T. Nozaki, K. Furukawa, Treatment of domestic sewage by a metal membrane bioreactor, Water Sci. Technol. 65(6) (2012) 1102–1108.

[6] P. Le-Clech, V. Chen, T.A.G. Fane, Fouling in membrane bioreactors used in wastewater treatment, J. Membr. Sci. 284 (2006) 17–53.

[7] G.J. Zhang, S.L. Ji, X. Gao, Z.Z. Liu, Adsorptive fouling of extracellular polymeric substances with polymeric ultrafiltration membranes, J. Membr. Sci. 309 (2008) 28–35.

[8] T. Zhu, Y.H. Xie, J. Jiang, Y.T. Wang, H.J. Zhang, T. Nozaki, Comparative study of polyvinylidene fluoride and PES flat membranes in submerged MBRs to treat domestic wastewater, Water Sci. Technol. 59(3) (2009) 399–405.

[9] N. Xu, W.H. Xing, N.P. Xu, J. Shi, Study on ceramic membrane bioreactor with turbulence promoter, Sep. Purif. Technol. 32 (2003) 403–410.

[10] S.T. Zhang, Y.B. Qu, Y.H. Liu, F.L. Yang, X.W. Zhang, K. Furukawa, Y. Yamada, Experimental study of domestic sewage treatment with a metal membrane bioreactor, Desalination 177 (2005) 83–93.

[11] R. Aryal, M.A.H. Johir, S. Vigneswaran, J. Kandasamy, R. Sleigh, Performance of a stainless steel membrane in membrane bioreactor process, Desalin. Water Treat. 41 (2012) 258–264.

[12] I.-J. Kang, S.-H. Yoon, C.-H. Lee, Comparison of the filtration characteristics of organic and inorganic membranes in a membrane-coupled anaerobic bioreactor, Water Res. 36 (2002) 1803–1813.

[13] A.D. Eaton, L.S. Clesceri, A.E. Greenberg, Standard Methods for the Examination of Water and Wastewater, 19th ed., American Public Health Association/American Water Works Association/Water Environment Federation, Washington, DC, 1995.

[14] J. Kanda, Determination of ammonium in seawater based on the indophenol reaction with O-phenylphenol (OPP), Water Res. 29(12) (1995) 2746–2750.

[15] J.H. Sun, Y. Pan, S.S. Huang, Study of critical flux in flat-sheet membrane bioreactors, J. Saf. Environ. 7(4) (2007) 39–41. (In Chinese).

[16] E.H. Bouhabila, R.B. Aïm, H. Buisson, Fouling characterisation in membrane bioreactors, Sep. Purif. Technol. 22–23 (2001) 123–132.

[17] J.H. Choi, H.Y. Ng, Effect of membrane type and material on performance of a submerged membrane bioreactor, Chemosphere 71 (2008) 853–859.

[18] P.J. Evans, M.R. Bird, A. Pihlajamäki, M. Nyström, The influence of hydrophobicity, roughness and charge upon ultrafiltration membranes for black tea liquor clarification, J. Membr. Sci. 313 (2008) 250–262.

[19] R.W. Field, D. Wu, J.A. Howell, B.B. Gupta, Critical flux concept for microfiltration fouling, J. Membr. Sci. 100 (1995) 259–272.

[20] Y. Ye, V. Chen, A.G. Fane, Modeling long-term subcritical filtration of model EPS solutions, Desalination 191 (2006) 318–327.

[21] M. Li, Y. Wang, C.P. Gong, Effect of on-line ultrasound on the properties of activated sludge mixed liquor and the controlling of membrane fouling in SMBR, Desalin. Water Treat. 51 (2013) 3938–3947.